A novel approach to oral iron delivery using ferrous sulphate loaded solid lipid nanoparticles

M.Gulrez Zariwala[a]
Naba Elsaid[b]
Timothy L. Jackson[c]
Francisco Corral López[b]
Sebastien Farnaud[d]
Satyanarayana Somavarapu[b]
Derek Renshaw[a]

[a] Department of Human & Health Sciences, University of Westminster
[b] Department of Pharmaceutics, UCL School of Pharmacy
[c] Department of Ophthalmology, King's College Hospital
[d] Department of Life Sciences, University of Bedfordshire

NOTICE: this is the author's version of a work that was accepted for publication in the International Journal of Pharmaceutics. Changes resulting from the publishing process, such as peer review, editing, corrections, structural formatting, and other quality control mechanisms may not be reflected in this document. Changes may have been made to this work since it was submitted for publication. A definitive version was subsequently published in the International Journal of Pharmaceutics, 456 (2). pp. 400-407, 18 November 2013. DOI 10.1016/j.ijpharm.2013.08.070

A novel approach to oral iron delivery using ferrous sulphate loaded solid lipid nanoparticles

M.Gulrez Zariwala [a], Naba Elsaid [b], Timothy L Jackson [c], Francisco C López [b], Sebastien Farnaud [d], Satyanarayana Somavarapu [b,†], Derek Renshaw [a,†,*]

[a] *School of Life Sciences, University of Westminster, 115 New Cavendish Street, London W1W 6UW, United Kingdom*

[b] *Department of Pharmaceutics, UCL School of Pharmacy, 29-39 Brunswick Square, London WC1N 1AX, United Kingdom*

[c] *Department of Ophthalmology, King's College Hospital, Denmark Hill, London SE5 9RS, United Kingdom*

[d] *Department of Life Sciences, University of Bedfordshire, Luton, Bedfordshire LU1 3JU, United Kingdom*

† **Authors contributed equally to this work**

*** Corresponding author:** D.renshaw1@westminster.ac.uk

School of Life Sciences, University of Westminster, 115 New Cavendish Street, London W1W 6UW, United Kingdom

Tel: 0044 (0)20 7911 5086
Fax: 0044 (0)20 7911 5087

1. Introduction

Iron deficiency and subsequent iron deficiency anaemia (IDA) are the most prevalent nutritional disorders worldwide (Zimmermann and Hurrell, 2011). The World Health Organisation (WHO) recently ranked iron deficiency as seventh in a list of top ten global preventable risks for death, disease and disability (Hurrell et al. 2004). Current strategies to counter iron deficiency include food iron fortification and iron supplementation (Zimmermann and Hurrell, 2007). Iron supplements are also administered prophylactically to pregnant women and low-birth weight infants. Both these interventions are heavily dependent on utilising ferrous iron based products. The iron salt ferrous sulphate ($FeSO_4$), first used as an iron supplement in the 19th century, is the most commonly used iron source in current use (Andrews, 1999; Crosby, 1984). Despite the development of several novel iron forms over the past decades ferrous sulphate remains the first choice, mainly due to its low cost (Martnez-Navarrete et al. 2002). Ferrous sulphate, however, is highly reactive and ferrous iron based supplements are known to cause adverse gastrointestinal (GI) effects on account of the unabsorbed free iron that accumulates in the gastric lumen and irritates the mucosa (Saha, Pandhi et al. 2007; Schümann et al. 2007). These lead to low patient compliance and therefore severely limit the benefits of iron supplementation therapy (Schümann et al. 2007).

These issues have led to the application of microencapsulation technology for oral iron delivery, wherein iron is incorporated within a lipid shell. The putative advantages are protecting the core ingredient from interacting with the other ingredients and to prevent the free iron from coming in direct contact with the GI mucosa thereby reducing the possibility of side effects

Solid lipid nanoparticles (SLN's) were first described by Muller et al, 1995 and have recently gained interest for drug delivery applications. SLN's retain the advantages of traditional liposome based formulations such as high absorption and biocompatibility, while overcoming issues of stability commonly encountered with liposomes (Souto and Müller, 2010). SLN's have been investigated for parenteral drug delivery and have successfully been demonstrated to possess good pharmacokinetics and tissue distribution characteristics when used for drugs such as doxorubicin and tobramycin (Bargoni et al. 2001; Zara et al. 2002). SLN based topical formulations have also been developed for cosmetic applications, and some products are already being marketed commercially (Castro, et al. 2009; Müller et al. 2002). Notably, SLN's have been investigated for oral drug delivery and have been shown to exhibit good release characteristics and systemic bioavailability of the encapsulated drugs (Demirel et al. 2001; Yang, et al. 1999). SLN tolerability and toxicity has also been characterised *in vivo* (Fundarò et al. 2000; Sanna et al. 2004) as well as *in vitro* (Müller et al. 1997; Mussi, et al. 2013; Nassimi, et al. 2010), and they are regarded to be generally well tolerated, owing to their composition from physiologically similar lipids.

In the current study, we examined the potential of SLN's for oral iron delivery. The aim of our study was to formulate SLN's incorporating the hydrophilic molecule ferrous sulphate ($FeSO_4$), and evaluate iron absorption from these *in vitro* using the well characterised human intestinal cell line Caco-2, with

intracellular ferritin formation as a marker of iron absorption (Fairweather-Tait et al. 2007). We also examined the influence of the mucoadhesive polysaccharide chitosan (Chi) incorporation onto the particles on physiochemical and iron absorption characteristics of the particles by preparing chitosan coated SLN's.

2. Material and methods:

2.1 Materials

Stearic acid and polyvinyl alcohol (PVA) were from Sigma-Aldrich (Dorset, UK). Chitosan hydrochloride (HCL) was purchased from Heppe Medical (Halle, Germany). Unless otherwise stated all chemicals and reagents used were also from Sigma-Aldrich (Dorset, UK). Caco-2 cells were purchased from European Collection of Cell Cultures (Catalogue no. 09042001, ECACC, Salisbury, UK). Cell culture media and foetal calf serum (FCS) were from Invitrogen (Loughborough, UK), and culture plates and flasks were from Nunc (Roskilde, Denmark). Ferritin ELISA kit (Product code S-22) was procured from Ramco (ATI Atlas, Chichester, UK) and protein assay kit (Product no. 23225) was from Pierce (Thermo Fisher Scientific, Northumberland, UK). To remove any traces of residual minerals all reagents were prepared using ultrapure water (MilliQ; resistivity of 18.2 MΩ cm), and glassware and utensils were soaked in 10% HCL and then rinsed with ultrapure water.

2.2 Methods

2.2.1 SLN preparation

Solid lipid nanoparticles were prepared using stearic acid by double emulsion solvent evaporation process. The preparation was based on methods described previously, with some modifications (Singh et al. 2010). Briefly, the oil phase was prepared by dissolving stearic acid (100 mg) in a 10 ml solvent mixture of dichlormethane and methanol (1:1 v/v) and pre-warming to 60 °C in a water bath. Aqueous emulsifier phase (PVA 10% w/v solution) with or without the addition of ferrous sulphate (1%, 2% or 3% w/w total lipid) was heated to equivalent temperature. Chitosan HCL (0.1%, 0.2%, or 0.4% w/v) was added to the aqueous phase to prepare chitosan coated SLN's. The aqueous phase and the oil phase were homogenised using an IKA UltraTurrax (IKA Labortechnik, Staufen, Germany) overhead stirrer (21,000 rpm, 60 °C, 4 mins) to obtain the primary emulsion which was then poured into 20 ml PVA (1% w/v) solution and homogenised again (21,000 rpm, 60 °C, 7 mins). The resultant double emulsion was rotary evaporated, cooled in an ice bath for 15 minutes and then washed twice followed by lyophilisation. SLN samples were lyophilised for 24 h (- 40°C) using a VirTis AdVantage 2.0 BenchTop freeze dryer (SP Industries, Ipswich, UK). This was followed by a secondary drying phase of 8 h (20 °C). SLN preparations were then assessed for physiochemical properties and optimised formulations with the most favourable characteristics were selected for comparative *in vitro*

analysis experiments (iron absorption and cytotoxicity). Composition of SLN formulations is shown in Table 1.

Table 1. Composition of solid lipid nanoparticle (SLN) formulations.

Formulation	Lipid Concentration (mg)	Iron concentration (% w/w lipid)	Chitosan concentration (% w/v)
SLN	100	-	-
SLN-FeA	100	1	-
SLN-FeB	100	2	-
SLN-FeC	100	4	-
SLN-ChiA	100	-	0.1
SLN-ChiB	100	-	0.2
SLN-ChiC	100	-	0.4
SLN-Fe-ChiA	100	1	0.1
SLN-Fe-ChiB	100	1	0.2
SLN-Fe-ChiC	100	1	0.4

2.2.2 Determination of iron incorporation efficiency

Iron incorporation in SLN's was determined by particle ultrafiltration followed by quantification based on methods described previously (Nepal et al. 2007; Ruckmani and Sankar, 2010). Briefly, SLN dispersions were centrifuged at high speed (13,000 rpm, 30 minutes, 4 °C); aliquots of the supernatant were then withdrawn and used to measure unincorporated iron spectrophotometrically using a modified ferrozine assay developed in our laboratory (Zariwala et al., in press). Aliquots of test samples and iron standards were pipetted into microcentrifuge tubes containing HCL (0.5 M). Detection reagent (2 mM ferrozine) was then added further and the tubes incubated in the dark for 60 mins. Ferrous iron binds with ferrozine to form a strongly coloured purple complex with an absorption maximum at 562 nm (Fish, 1988). Samples were pipette into a 96-well microplate and absorbance read at 562 nm using a microplate reader (VersaMax, Molecular devices, USA). Iron content in test samples was calculated from the standard curve generated from the iron standards.

Mean of three independent readings were recorded and results were expressed as means ± standard deviations (SD).

Iron incorporation in SLN's was determined according to the following equation:

Iron incorporation efficiency (%) = $(Ti - Fi / Ti) \times 100$

Where T*i* is the total iron added during formulation and F*i* is the free (unincorporated) iron measured in supernatant.

2.2.3 SLN characterisations

2.2.3.1 Particle size measurements

Size analysis was carried out on SLN dispersions as well as lyophilised SLN samples using the Malvern Zetasizer Nano ZS (Malvern Instruments, UK), carrying out three measurements on each sample. Results were analysed using the Fraunhofer model and presented as mean particle size ± SD.

2.2.3.2 Zeta potential analysis

Zeta potential analysis of SLN's was carried out on dispersions diluted in MilliQ water; all measurements were replicated in triplicate. Electrophoretic mobility of the dispersions was then measured by laser doppler anemometry (Zetasizer Nano ZS, Malvern Instruments, UK).

2.2.3.3 SLN imaging

Drop's of SLN dispersions were applied to a copper grid and stained with 2% phosphotungstic acid solution. SLN's were then imaged using a Philips Biotwin CM120 transmission electron microscope (TEM; Philips Biotwin CM120, Philips Co, The Netherlands).

2.2.4 Thermal analysis of SLN using differential scanning calorimetry (DSC)

Thermal analysis of pure compounds (ferrous sulphate and stearic acid), and lyophilised SLN preparations was carried out using differential DSC (DSC Q2000 module, TA Instruments, LLC, USA). Aluminium hermetic pans containing a 50 µm pinhole were used to load the lyophilised preparations pans (TA Instruments, New Castle, UK) as described previously (Slager and Prozonic, 2005). A heating rate of 20 °C per min was employed in the 0–300 °C range under nitrogen atmosphere at a flow rate of 50 ml/min.

2.2.5 Cytotoxicity assay

SLN cytotoxicity was assessed using an MTT (3-(4,5-dimethylthiazol-2-yl)-2,5-diphenyl-tetrazolium bromide) assay (Mosmann, 1983; Silva et al. 2011). Briefly, Caco-2 cells were seeded onto 96-well plates at a seeding density of 3×10^4 cells/cm^2 and media replenished every 48 hours. Growth media was then aspirated and cells incubated for 48 or 72 hours with test media comprising of phenol red

free Dulbecco's Modified Eagle Medium (DMEM) supplemented with SLN's at volumes equivalent to final iron concentrations of 20, 50 and 100 µM. Corresponding blank SLN formulations were added at equivalent volumes. Following incubation periods, cells were solubilised in dimethyl sulfoxide (DMSO) and the absorbance measured in a plate reader (VersaMax, Molecular devices, USA) at 550 nm wavelength. Cell viability was expressed as a percentage of untreated control cells (100%).

2.2.6 Caco-2 cell iron absorption

Caco-2 cells (passage no. 45 to 55) were seeded onto 6-well plates at an initial seeding density of 3 x 10^4 cells/cm^2. Parallel 6-well plates were also seeded similarly to be used for assessment of cell viability prior to the commencement of the absorption experiment and following completion. Cells were cultured in an incubator at 37 °C in an atmosphere of 95 % air and 5 % CO_2 at constant humidity, replacing the medium (FCS supplemented DMEM; Dulbecco's Modified Eagle Medium) every two days. Caco-2 cells differentiate to a fully matured gastrointestinal (GI) tract phenotype 14-15 post seeding. Day 13 - cell monolayers were incubated in serum-free minimum essential media (MEM) for 24 hours after washing times with wash solution (140 mM NaCl, 5 mM KCl, 10 mM PIPES buffer, pH 6.7, 37ºC). Day 14 - Treatment media was prepared by adding SLN samples (20 µM final iron concentrations) to aliquots of test media (MEM, pH 5.8, buffered with 2-[N-Morpholino] ethanesulfonic acid 10 mM). Caco-2 cell monolayers were washed three times with wash solution and iron enriched treatment media was added to cell monolayers (n = 6 wells per condition). Plates were incubated for 2 hours at 37ºC on a rotating plate incubator (25 rpm). Test media was then aspirated and cells washed twice with wash solution and once with surface bound iron removal solution (wash solution plus 5 µm Na hydrosulphite and 1 µm bathophenanthroline disulfonate) (Glahn et al. 1995). Cells were then placed in a cell culture incubator for 24 h after which they were subjected to lysis (50 mM NaOH supplemented with 1 µg/ml protease inhibitor cocktail (Sigma-Aldrich product # P8340) followed by harvesting (using a cell scraper) and collecting the lysate into microcentrifuge tubes.

2.2.6.1 Iron absorption analysis

Iron absorption was determined by measuring total ferritin protein concentration in cell lysates using a spectrophotometric ELISA kit as described previously (Zariwala et al., in press; Thompson et al. 2010). BCA protein assay kit (Thermo Fisher Scientific (Northumberland, UK) was used to determine total protein content of Caco-2 cell lysates. Samples were assayed in duplicate following manufacturer's protocol using bovine serum albumin (BSA) stock (2 mg/ml) as a standard. Absorbance was measured at 562 nm using a microplate reader (VersaMax, Molecular devices, USA). Ferritin concentration was then standardised against total protein concentration (ng ferritin/mg protein) and considered a marker of iron absorption.

2.2.7 Statistical analysis

For iron absorption experiments mean of six replicates was calculated for each treatment, and the data presented as mean ± SD. All data was analysed by ANOVA followed by Tukey's *post-hoc* test using the PRISM software package (Version 4, Graphpad Software Inc., San Diego, USA). In all cases results were considered significantly different if $p \leq 0.05$.

3. Results and Discussion

3.1 Effect of initial iron content on SLN iron incorporation efficiency.

A preliminary experiment was carried out to optimise initial iron concentration in the SLN formulations. The formulations were therefore prepared using varying iron concentrations (1%, 2% and 4% w/w lipid) and SLN incorporation efficiencies determined. Our results demonstrate that increasing initial iron concentration from 1% to 2% and 2% to 4% w/v resulted in a 29.57% ($p < 0.01$) and 21.12% ($p < 0.05$) decrease (respectively) in iron incorporation efficiency of the lipid particles (Fig. 1). This is in agreement with previous studies in liposomes by Xia and Xu (2005), where an inverse relationship was observed between increasing iron to lipid content and liposome iron entrapment (Xia and Xu, 2005). Factors that influence SLN drug incorporation include solubility and miscibility of the drug in the lipid melt, physiochemical interactions between the drug and encapsulating material, and formulation parameters such as homogenisation amplitude time (Mehnert and Mäder, 2001). It has been suggested that the strong electrolytic properties of ferrous iron might have a detrimental effect on the lipid vesicle wall formation (Hermida et al. 2010; Xia and Xu, 2005). High initial iron concentration may also lead to lower solubility in the lipid melt thereby impairing incorporation into the lipid.

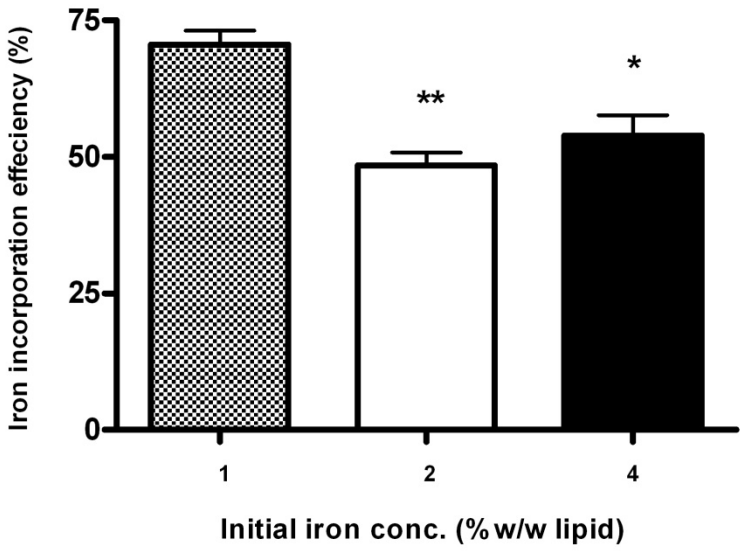

Fig. 1. Effect of initial iron concentration (% w/w lipid) upon solid lipid nanoparticle (SLN) iron incorporation efficiency. Results are expressed as mean ± SD (*n* =3). ** signifies $p < 0.01$ and * signifies $p < 0.05$.

The initial amount of ferrous iron added to the SLN formulations was thus optimised at 1% w/w of the total lipid. A second batch of formulations was prepared with this optimised iron concentration (1% w/w total lipid) to investigate the effect of chitosan inclusion upon SLN iron incorporation. Chitosan-HCL was used at concentrations of 0.1%, 0.2% and 0.4% w/v. Chitosan inclusion at 0.2% w/v concentration was observed to result in a statistically significant increase in SLN iron incorporation as compared to SLN-Fe alone ($p < 0.05$, Fig. 2). However, increasing chitosan concentration from 0.2% to 0.4% w/v did not result in a significant increase in iron incorporation efficiency (Fig.2). Inclusion of chitosan has been shown previously to result in increased iron loading in lipid vesicles (Hermida et al. 2010; Xia and Xu, 2005). It has been suggested that iron forms a stable complex with the lipid associated chitosan, resulting in higher incorporation (Bhatia and Ravi, 2003).

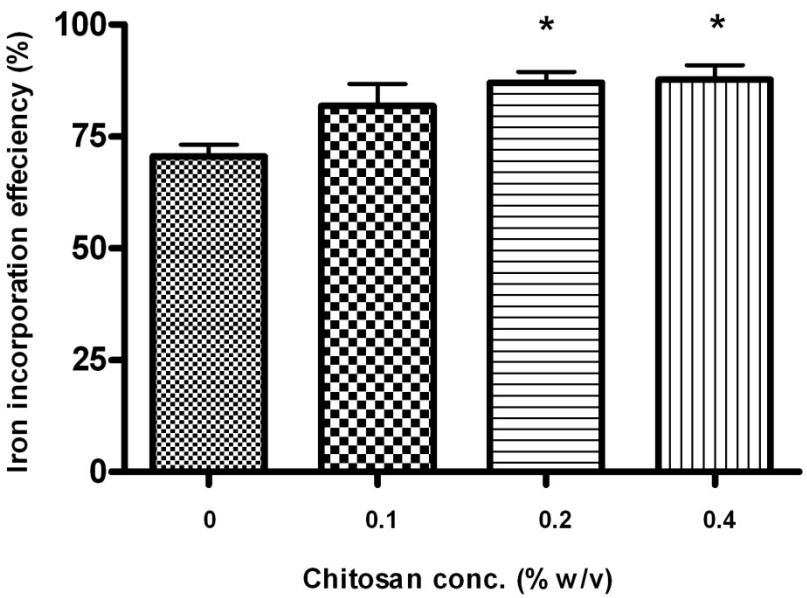

Fig. 2. Effect of chitosan inclusion on solid lipid nanoparticle (SLN) iron incorporation efficiency. Results are mean ± SD (*n* = 3). * Indicates significant difference from chitosan free SLN.

3.2 Physiochemical properties of SLN's

Particle size distribution and zeta potential of SLN's are shown in Table 1. Mean particle size of all SLN's was of submicron dimensions (300.3 ± 31.75 nm to 495.1 ± 80.42 nm). Lyophilisation led to a moderate increase in SLN particle size. The presence of iron did not result in any significant changes in SLN particle size (Table 2). Chitosan inclusion however did lead to a significant increase in particle size as compared to chitosan free SLN formulations (Table 2).

Generally, an inverse relationship is observed between the emulsifier concentration and the size of the lipid particles (Lim and Kim, 2002). We optimised PVA emulsifier concentration at 10 % w/v, as this concentration, along with formulation parameters (temperature and homogenisation time) resulted in particles within our desired size range. Very small sized SLN's (sub 200 nm) are favoured for drug delivery applications such as anti-cancer drugs and for targeted delivery across the blood brain barrier (BBB), where high drug penetration and retention is desirable (Chen and Liu, 2012; Kaur et al. 2008; Oyewumi, et al. 2004). In the case of these delivery systems, the small size of the particles is considered advantageous to avoid reticoendothelial clearance (Chen and Liu, 2012). However, for oral iron delivery our objective was to formulate iron loaded particles that follow the conventional mode of iron absorption; i.e. via controlled entry through the intestinal enterocytes.

Table 2. Physiochemical properties of solid lipid nanoparticles (SLN). All values are mean ± SD (n = 3).

Formulation	Size (nm) Before lyophilisation	Size (nm) After lyophilisation	Zeta potential (mV)	Iron incorporation efficiency (%)
SLN	369.1 ± 43.2	604.93 ± 64.6	-10.3 ± 3.4	-
SLN-FeA	333.7 ± 55.4	516.27 ± 67.2	-12.2 ± 1.9	70.57 ± 4.5
SLN-FeB	300.3 ± 31.8	306.77 ± 37.8	-15.8 ± 0.2	48.48 ± 4.0
SLN-FeC	331.3 ± 27.6	312.47 ± 4.8	-17.8 ± 1.8	53.92 ± 6.5
SLN-ChiA	546.9 ± 66.7	651.3 ± 167.2	3.43 ± 0.2	-
SLN-ChiB	716.7 ± 88.9	750.2 ± 87.6	3.59 ± 0.8	-
SLN-ChiC	655.0 ± 100.1	948.0 ± 110.4	7.82 ± 0.6	-
SLN-Fe-ChiA	554.2 ± 78.7	602.2 ± 64.8	5.55 ± 0.5	81.84 ± 8.5
SLN-Fe-ChiB	495.1 ± 80.4	788.6 ± 250.6	6.90 ± 1.8	87.01 ± 4.2
SLN-Fe-ChiC	690.2 ± 78.1	736.4 ± 146.9	10.7 ± 0.1	87.70 ± 5.7

Zeta potential analysis indicates particle surface charge, and is considered predictive of formulation stability, particularly for emulsions and colloidal suspensions (Heurtault et al. 2003). Stearic acid SLN's had a net negative surface charge, in agreement with previous studies (Wang et al. 2012). In all cases, iron incorporation did not significantly alter particle surface charge, as indicated by the comparison of zeta potential between blank and corresponding iron loaded SLN's. Chitosan conferred a net positive charge on the surface of the lipid particles, with increasing chitosan concentrations (from 0.1% to 0.4% w/v) leading to a corresponding increase in surface charge (Table 2.). An overall net positive zeta potential of the lipid particles leads to electric repulsion between the particles

reducing the likelihood of aggregation (Heurtault et al. 2003). Positively charged particles are also known to exhibit greater cellular binding and consequent cellular uptake (Yu et al. 2012).

SLN surface and shape characteristics were visualised by TEM (Fig. 3.). The imaging confirms the uniformly well formed spherical shape and structures of the SLN's. Particles appear free from aggregation further confirming the stable formulation characteristics of the SLN's.

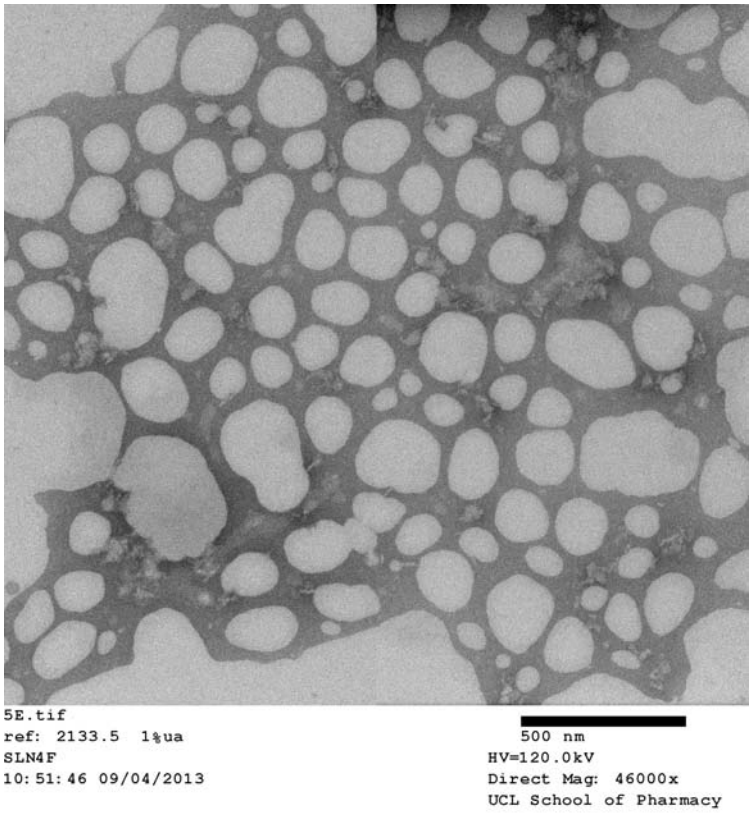

Fig. 3. Transmission electron microscopy (TEM) image of iron loaded SLN-Chi-FeB visualised at 46,000x magnification.

3.3 Thermal properties of SLN's.

DSC was used to analyze the thermophysical properties of SLN's and their individual components (e.g. stearic acid and ferrous sulphate) to study changes which may result from particle formation and component interaction. Stearic acid was shown to exhibit a bifurcated peak with melting points at 60.55 °C and 71.22 °C (Fig. 4A) indicating that the unmodified stearic acid used in this study has crystalline properties, in agreement with previous studies (Cavalli et al., 1997).The bifurcated peak may indicate the presence two crystalline polymorphic forms of which the less stable polymorph (at 60.55 °C) disappears in the blank SLN formulations suggesting a decline in the crystallinity of stearic acid upon SLN formation (Fig 4A). Ferrous sulphate showed the presence of three endorthermic peaks (76.09 °C, 106.5 °C and 124.64 °C) indicating its crystalline properties (Fig. 4B). All three

ferrous peaks disappeared in the diffractograms of ferrous iron loaded SLN particles (Fig 4B) suggesting that ferrous sulphate interacts with the SLN components during the formulation process and this gives rise to a SLN crystal structure that is distinct from that of individual components. Previous studies in SLN's have demonstrated that during formulation the lipid components undergo arrangements into lamellar lattice structures, and crystalline compounds are incorporated and stored within these layers (Lukowski et al. 2000).Our DSC data therefore suggest that ferrous sulphate is successfully incorporated within the lipid matrix of the SLN's during the formulation process and is in agreement with the results of our iron incorporation efficiency experiments.

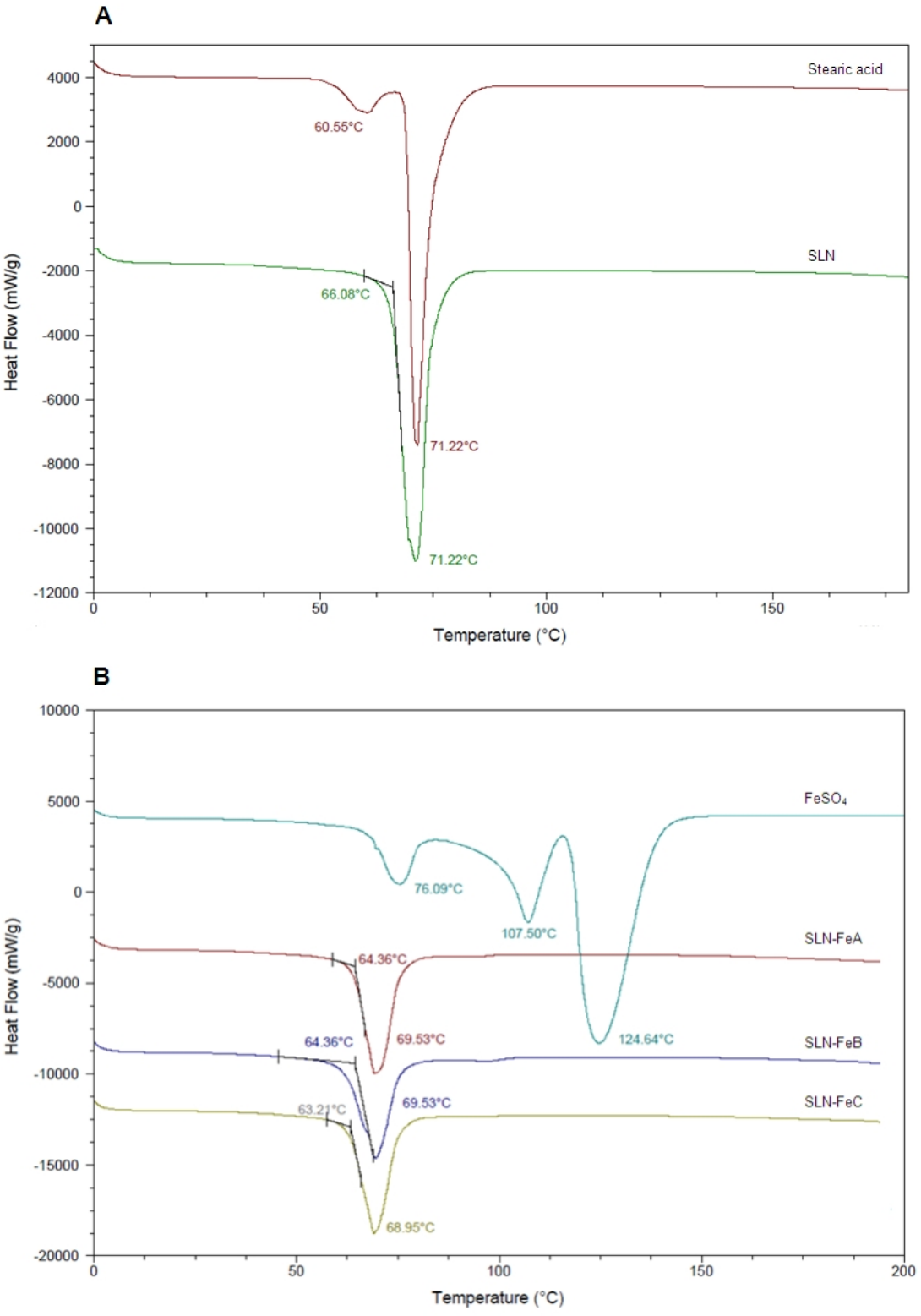

Fig. 4. Thermal analysis of solid lipid nanoparticles (SLN's). A: DSC thermograms of stearic acid and blank SLN. B: DSC thermogram of ferrous sulphate ($FeSO_4$) loaded SLN formulations (SLN-FeA, SLN-FeB, SLN-FeC).

SLN formulations were selected for in-depth *in vitro* analysis in Caco-2 cells based on the results of the characterisation analysis. SLN iron concentration was selected at 1% w/w lipid as this concentration resulted in the highest incorporation efficiency and likewise, the chitosan concentration was selected at 0.2% w/v as SLN formulations at this concentrations demonstrated a favourable balance between requisite size, charge and iron incorporation properties. Thus iron containing SLN-FeA and SLN-Fe-ChiB and their corresponding blank SLN formulations SLN and SLN-ChiB were assessed in our *in vitro* experiments for cytotoxicity and iron uptake.

3.4 SLN cytotoxicity analysis

Although SLN formulation ingredients were carefully selected, there might be concerns regarding SLN effect on cell viability either upon contact with the cell membrane or following cellular entry. We sought to address this by carrying out SLN cytotoxicity analysis in Caco-2 cells using the well characterised MTT assay. Caco-2 cells were exposed to SLN formulations standardised at increasing iron concentrations (20, 50 and 100 μM), with corresponding iron free SLN formulations also included, and cytotoxicity assessed at two time points (48h and 72h). Our results demonstrate that none of the SLN formulations exerted any potential cytotoxic effects on Caco-2 cells at any time point (Fig 5). Cell viability in all cases was at least 80% of control cells (Fig. 5). Our results therefore demonstrate the absence of any cytotoxic effects and further underpin the potential of our SLN formulations for oral iron delivery.

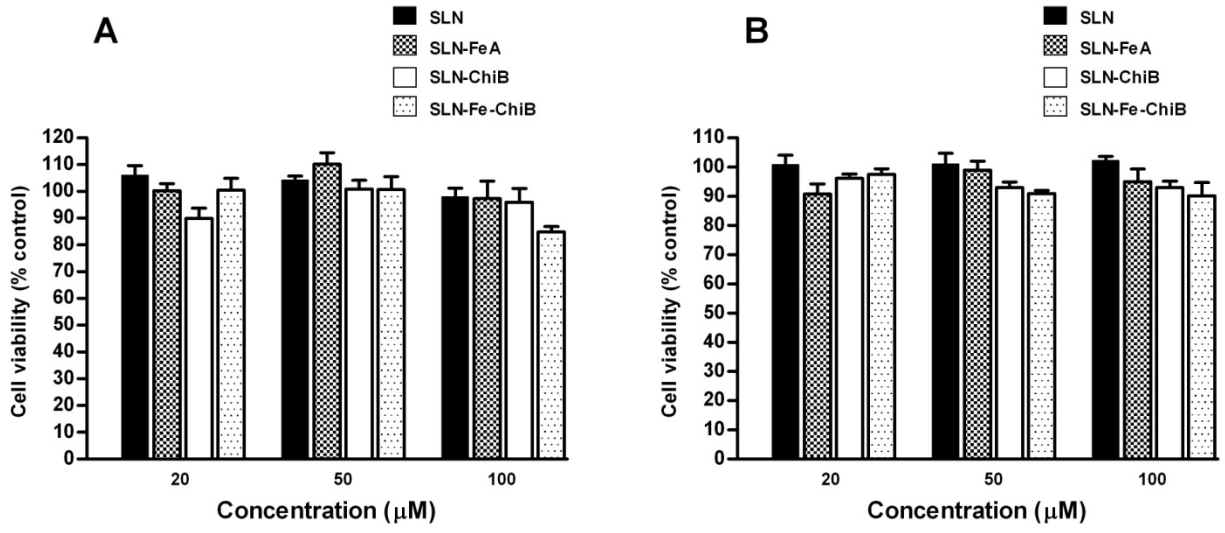

Fig. 5. SLN cytotoxicity analysis. Caco-2 cells viability was assessed by MTT assay following incubation with SLN formulations for 48 and 72 h at varying iron concentrations (20 μM, 50 μM and 100 μM), with corresponding blank SLN formulations included at equivalent volumes. Results are mean ± SD (*n* = 6).

3.5 SLN iron absorption in Caco-2 cells

Our results demonstrate significantly higher iron absorption from SLN formulations. Iron absorption from SLN-FeA (583.98 ± 40.83 ng/mg) was 13.42% higher than free ferrous sulphate reference whereas for SLN-Fe-ChiB (642.77 ± 29.37 ng/mg) it was 24.9% higher than the ferrous sulphate reference ($p < 0.05$). The chitosan coated formulation SLN-Fe-ChiB demonstrated the overall highest iron absorption (514.66 ± 20, $p < 0.05$). The high lipid content of the SLN formulations offers a possible explanation to account for the enhanced iron absorption profile observed from these formulations as compared to free iron. Lipids are known to enhance intestinal absorption of entrapped or co-administered drugs via several putative mechanisms, and several studies have reported lipid mediated enhancement of absorption and bioavailability of both lipophilic and hydrophilic drugs including zidovudine (Singh et al. 2010), tretinoin (Das et al. 2011) and puerarin (Luo et al. 2011). The inherent lipophilic nature of lipid-based systems promotes particle transport across the bimolecular lipid membrane of most mammalian cells such as gut enterocytes (Eldridge et al. 1990). Lipid particles are also known to exhibit bioadhesive properties, which allow them to adhere to the GI tract thereby increasing the likelihood of cellular uptake (Severino et al. 2012). Lipids might also function as permeability enhancers that modify the barrier function of the GI tract (Aungst, 2000). Some studies have suggested that lipids enhance intestinal bioavailability of drugs by attenuating efflux transporters, such as p-glycoprotein located on the apical intestinal mucosa (Constantinides and Wasan, 2007; Dintaman and Silverman, 1999). Stearic acid, a long chain fatty acid, was used as the lipid phase in our formulations. Stearic acid has been used extensively to prepare SLN's for various drugs and bioactives (Guan et al. 2011; Yuan et al. 2007; Zhang et al. 2000). Despite being a saturated fatty acid it has not been shown to causes adverse changes in serum cholesterol levels (Grundy, 1994). Our choice of stearic acid as the lipid component was further reinforced on account of its United States Food and Drug Administration Generally Recognised as Safe (USFDA GRAS) status as a food additive (U.S. FDA Code of Federal Regulations), suggestive of a good biocompatibility profile (Osborn and Akoh, 2002).

Iron absorption from SLN's was determined by measuring Caco-2 cell ferritin formation (Zariwala et al., in press). Ferritin is an iron storage protein that is widely considered a marker of iron absorption (Andrews, 1999), and the Caco-2 ferritin model has been well characterised for *in vitro* iron absorption studies (Alvarez-Hernandez et al. 1991). Several studies have also demonstrated physiologically relevant iron uptake and synthesis machinery in this cell system (Fairweather-Tait et al. 2007). Caco-2 cells are known to synthesise ferritin based on their intracellular iron levels and iron concentrations in their surrounding environment (Sharp, 2005). Cells were therefore cultured in iron depleted media for 24 h prior to experiments and then incubated with equivalent amounts of iron (20 μm) from the test formulations for two hours. The test iron concentration and the incubation time were based on previous studies that have demonstrated these parameters to be optimum for comparative iron uptake studies (Sharp, 2005).

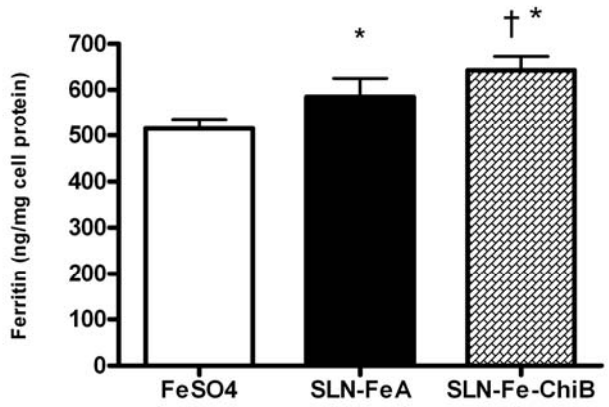

Fig. 6. Caco-2 cell iron absorption from test SLN formulations. Results are shown as mean ± SD (n = 6), * indicates a significant difference between ferrous sulphate control and SLN-FeA ($p < 0.05$). † indicates significant difference between SLN-FeA and SLN-Chi-FeB ($p < 0.05$).

Chitosan integration in our SLN's led to markedly augmented Caco-2 cell iron absorption. Chitosan is known to function as an absorption enhancer when included in micro and nano-particle formulations, an effect attributed to its mucoadhesive properties that have been well described (Fonte et al. 2011). The apical surface of duodenal enterocytes is coated with a glycocalyx layer that possesses a net negative charge (Snoeck et al. 2005). Chitosan has a strong positive charge owing to the presence of amine groups in its structure; this leads to strong electrostatic attraction with the cell surface and subsequent bioadherence that is conducive to increased absorption. Other groups have also demonstrated similar results; Takeuchi and colleagues (2003) reported increased enterocyte uptake of calcitonin loaded liposomes surface coated with chitosan, while Fonte et al. (2011) recently showed high oral absorption from chitosan coated solid lipid particles (Fonte et al. 2011; Takeuchi et al. 2003). As described earlier, chitosan inclusion also led to increased iron incorporation and modification of the surface charge of the lipid particles. Chitosan inclusion in the SLN's therefore leads to markedly higher iron absorption from SLN; an effect we attribute to its mucoadhesive and permeation enhancing properties that might further supplement the cellular uptake properties of the SLN vehicle.

4. Conclusion

We demonstrate, for the first time, the preparation of ferrous iron loaded SLN's as a platform for iron delivery. SLN preparation was optimised for initial iron content and surface charge, and these parameters were demonstrated to have a profound influence on their physiochemical and *in vitro* iron absorption characteristics. Our results show Caco-2 cell iron absorption from SLN's at levels higher than free ferrous sulphate. Inclusion of chitosan at an optimised concentration of 0.2% w/v imparted a net positive charge on the particle surface and led to a further augmentation of iron absorption from SLN's. In conclusion, we have developed a lipid-based oral iron delivery system with good iron incorporation and physiochemical characteristics as well as high absorption properties *in vitro*. Iron

loaded SLN's offer a versatile drug delivery system; they can be administered as nanodispersions, in powdered form (upon lyophilisation), and as a tableting ingredient to be added during the granulation process. Iron containing SLN's thus provide an attractive delivery system for conventional oral iron therapy.

Conflict of interest

The authors report no conflicts of interest.

Acknowledgements

MGZ and DR were supported by Early Career Grants from the Society for Endocrinology. The authors wish to thank Jenny Mackenzie, Head of the Dept of Human & Health Sciences, University of Westminster for funding MGZ during the experimental and writing stages of this manuscript.

References

Alvarez-Hernandez,X., Nichols,G.M., Glass,J., 1991. Caco-2 cell line: a system for studying intestinal iron transport across epithelial cell monolayers. Biochimica et Biophysica Acta (BBA) - Biomembranes, 1070, 205-208.

Andrews,N.C., 1999. Disorders of Iron Metabolism. N Engl J Med, 341, 1986-1995.

Aungst,B.J., 2000. Intestinal permeation enhancers. J. Pharm. Sci., 89, 429-442.

Bargoni,A., Cavalli,R., Zara,G.P., Fundarò., Caputo,O., Gasco,M.R., 2001. Transmucosal transport of tobramycin incorporated in solid lipid nanoparticles (SLN) after duodenal administration to rats. Part II – Tissue distribution. Pharmacological Research, 43, 497-502.

Bhatia,S.C., Ravi,N., 2003. A Mössbauer Study of the Interaction of Chitosan and d-Glucosamine with Iron and Its Relevance to Other Metalloenzymes. Biomacromolecules, 4, 723-727.

Castro,G.A., Coelho, A.L.Z., Oliveira,C.A., Mahecha,G.A.B., Oréficec.,R.L., Ferreira,L.A.M., 2009. Formation of ion pairing as an alternative to improve encapsulation and stability and to reduce skin irritation of retinoic acid loaded in solid lipid nanoparticles. International Journal of Pharmaceutics, 381, 77-83.

Cavalli,R., Caputo,O., Carlotti,M.E., Trotta,M., Scarnecchia,C., Gasco,M.R., 1997. Sterilization and freeze-drying of drug-free and drug-loaded solid lipid nanoparticles. International Journal of Pharmaceutics, 148, 47-54.

Chen,Y., Liu,L., 2012. Modern methods for delivery of drugs across the blood–brain barrier. Advanced Drug Delivery Reviews, 64, 640-665.

Constantinides,P.P., Wasan,K.M., 2007. Lipid formulation strategies for enhancing intestinal transport and absorption of P-glycoprotein (P-gp) substrate drugs: In vitro/In vivo case studies. J. Pharm. Sci., 96, 235-248.

Crosby,W.H., 1984. The rationale for treating iron deficiency anemia. Archives of Internal Medicine, 144, 471-472.

Das,S., Ng,W.K., Kanaujia,P., Kim,S., Tan,R.B.H., 2011. Formulation design, preparation and physicochemical characterizations of solid lipid nanoparticles containing a hydrophobic drug: Effects of process variables. Colloids and Surfaces B: Biointerfaces, 88, 483-489.

Demirel,M., Yazan,Y., Müller.,R.H., Kiliç.,F., Bozan,B., 2001. Formulation and in vitro-in vivo evaluation of piribedil solid lipid micro- and nanoparticles. J Microencapsul, 18, 359-371.

Dintaman,J., Silverman,J., 1999. Inhibition of P-Glycoprotein by D-alpha-Tocopheryl Polyethylene Glycol 1000 Succinate (TPGS). Pharmaceutical research, 16, 1550-1556.

Eldridge,J.H., Hammond,C.J., Meulbroek,J.A., Staas,J.K., Gilley,R.M., Tice,T.R., 1990. Controlled vaccine release in the gut-associated lymphoid tissues. I. Orally administered biodegradable microspheres target the peyer's patches. Journal of Controlled Release, 11, 205-214.

Fairweather-Tait,S., Phillips,I., Wortley,G., Harvey,L., Glahn,R., 2007. The use of solubility, dialyzability, and Caco-2 cell methods to predict iron bioavailability. Int. J. Vitam. Nutr. Res., 77, 158-165.

Fish,W.W., 1988. Rapid colorimetric micromethod for the quantitation of complexed iron in biological samples. Methods Enzymol, 158, 357-364.

Fonte,P., Nogueira,T., Gehm,C., Ferreira,D., Sarmento,B., 2011. Chitosan-coated solid lipid nanoparticles enhance the oral absorption of insulin. Drug Deliv. and Transl. Res., 1, 299-308.

Fundarò .A., Cavalli,R., Bargoni,A., Vighetto,D., Zara,G.P., Gasco,M.R., 2000. Non-stealth and stealth solid lipid nanoparticles (SLN) carrying doxorubicin: pharmacokinetics and tissue distribution after i.v. administration to rats. Pharmacological Research, 42, 337-343.

Glahn,R.P., Gangloff,M.B., Van Campen,D.R., Miller,D.D., Wien,E.M., Norvell,W.A., 1995. Bathophenanthrolene disulfonic acid and sodium dithionite effectively remove surface-bound iron from Caco-2 cell monolayers. J Nutr, 125, 1833-1840.

Grundy,S.M., 1994. Influence of stearic acid on cholesterol metabolism relative to other long-chain fatty acids. The American Journal of Clinical Nutrition, 60, 986S-990S.

Guan,Q., Guan,Q., Lin,T., Yin,J., 2011. Preparation and pharmacokinetics of solid lipid nanoparticles loaded with pueraria flavones. Journal of Controlled Release, 152, Supplement 1, e25-e26.

Hermida,L.G., Roig,A., Bregni,C., Sabés-Xamaní.M., Barnadas-Rodríguez,R., 2010. Preparation and characterization of iron-containing liposomes: their effect on soluble iron uptake by Caco-2 cells. Journal of Liposome Research, 21, 203-212.

Heurtault,B., Saulnier,P., Pech,B., Proust,J.E., Benoit,J.P., 2003. Physico-chemical stability of colloidal lipid particles. Biomaterials, 24, 4283-4300.

Hurrell,R.F., Lynch,S., Bothwell,T., Cori,H., Glahn,R., Hertrampf,E., Kratky,Z., Miller,D., Rodenstein,M., Streekstra,H., Teucher,B., Turner,E., Yeung,C.K., Zimmermann,M.B., null, 2004. Enhancing the absorption of fortification iron. A SUSTAIN Task Force report. Int J Vitam Nutr Res, 74, 387-401.

Kaur,I.P., Bhandari,R., Bhandari,S., Kakkar,V., 2008. Potential of solid lipid nanoparticles in brain targeting. Journal of Controlled Release, 127, 97-109.

Lim,S.J., Kim,C.K., 2002. Formulation parameters determining the physicochemical characteristics of solid lipid nanoparticles loaded with all-trans retinoic acid. International Journal of Pharmaceutics, 243, 135-146.

Lukowski,G., Kasbohm,J., Pflegel,P., Illing,A., Wulff,H., 2000. Crystallographic investigation of cetylpalmitate solid lipid nanoparticles. International Journal of Pharmaceutics, 196, 201-205.

Luo,C.F., Yuan,M., Chen,M.S., Liu,S.M., Zhu,L., Huang,B.Y., Liu,X.W., Xiong,W., 2011. Pharmacokinetics, tissue distribution and relative bioavailability of puerarin solid lipid nanoparticles following oral administration. International Journal of Pharmaceutics, 410, 138-144.

Müller,R.H., Radtke,M., Wissing,S.A., 2002. Solid lipid nanoparticles (SLN) and nanostructured lipid carriers (NLC) in cosmetic and dermatological preparations. Advanced Drug Delivery Reviews, 54, Supplement, S131-S155.

Müller,R., Rühl,D., Runge,S., Schulze-Forster,K., Mehnert,W., 1997. Cytotoxicity of Solid Lipid Nanoparticles as a Function of the Lipid Matrix and the Surfactant. Pharmaceutical research, 14, 458-462.

Martnez-Navarrete, N., Camacho, M. M., Martnez-Lahuerta, J., Martnez-Monzo, J., and Fito, P. Iron deficiency and iron fortified foods-a review. Food Research International 35[2], 225-231. 2002.
Ref Type: Abstract

Mehnert,W., Mäder,K., 2001. Solid lipid nanoparticles: Production, characterization and applications. Advanced Drug Delivery Reviews, 47, 165-196.

Mosmann,T., 1983. Rapid colorimetric assay for cellular growth and survival: Application to proliferation and cytotoxicity assays. Journal of Immunological Methods, 65, 55-63.

Mussi,S.V., Silva,R.C., Oliveira,M.N.C.D., Lucci,C.M., Azevedo,R.B.D., Ferreira,L.A.N.M., 2013. New approach to improve encapsulation and antitumor activity of doxorubicin loaded in solid lipid nanoparticles. European Journal of Pharmaceutical Sciences, 48, 282-290.

Nassimi,M., Schleh,C., Lauenstein,H.D., Hussein,R., Hoymann,H.G., Koch,W., Pohlmann,G., Krug,N., Sewald,K., Rittinghausen,S., Braun,A., Müller-Goymann,C., 2010. A toxicological evaluation of inhaled solid lipid nanoparticles used as a potential drug delivery system for the lung. European Journal of Pharmaceutics and Biopharmaceutics, 75, 107-116.

Nepal,P.R., Chun,M.K., Choi,H.K., 2007. Preparation of floating microspheres for fish farming. International Journal of Pharmaceutics, 341, 85-90.

Osborn,H.T., Akoh,C.C., 2002. Structured Lipids-Novel Fats with Medical, Nutraceutical, and Food Applications. Comprehensive Reviews in Food Science and Food Safety, 1, 110-120.

Oyewumi,M.O., Yokel,R.A., Jay,M., Coakley,T., Mumper,R.J., 2004. Comparison of cell uptake, biodistribution and tumor retention of folate-coated and PEG-coated gadolinium nanoparticles in tumor-bearing mice. Journal of Controlled Release, 95, 613-626.

Ruckmani,K., Sankar,V., 2010. Formulation and optimization of Zidovudine niosomes. AAPS PharmSciTech, 11, 1119-1127.

Saha,L., Pandhi,P., Gopalan,S., Malhotra,S., Saha,P.K., 2007. Comparison of efficacy, tolerability, and cost of iron polymaltose complex with ferrous sulphate in the treatment of iron deficiency anemia in pregnant women. MedGenMed., 9, 1.

Sanna,V., Kirschvink,N., Gustin,P., Gavini,E., Roland,I., Delattre,L., Evrard,B., 2004. Preparation and in vivo toxicity study of solid lipid microparticles as carrier for pulmonary administration. AAPS PharmSciTech, 5, e27.

Schümann ,K., Ettle,T., Szegner,B., Elsenhans,B., Solomons,N.W., 2007. On risks and benefits of iron supplementation recommendations for iron intake revisited. Journal of Trace Elements in Medicine and Biology, 21, 147-168.

Severino,P., Andreani,T., Macedo,A.S., Fangueiro,J.F., Santana,M.H., Silva,A.M., Souto,E.B., 2012. Current State-of-Art and New Trends on Lipid Nanoparticles (SLN and NLC) for Oral Drug Delivery. J Drug Deliv, 2012, 750891.

Sharp,P., 2005. Methods and options for estimating iron and zinc bioavailability using Caco-2 cell models: benefits and limitations. Int. J. Vitam. Nutr. Res., 75, 413-421.

Silva,A.C., González-Mira,E., García,M.L., Egea,M.A., Fonseca,J., Silva,R., Santos,D., Souto,E.B., Ferreira,D., 2011. Preparation, characterization and biocompatibility studies on risperidone-loaded solid lipid nanoparticles (SLN): High pressure homogenization versus ultrasound. Colloids and Surfaces B: Biointerfaces, 86, 158-165.

Singh,S., Dobhal,A.K., Jain,A., Pandit,J.K., Chakraborty,S., 2010b. Formulation and Evaluation of Solid Lipid Nanoparticles of a Water Soluble Drug: Zidovudine. Chemical and Pharmaceutical Bulletin, 58, 650-655.

Slager,T.L., Prozonic,F.M., 2005. Simple methods for calibrating IR in TGA/IR analyses. Thermochimica Acta, 426, 93-99.

Snoeck,V., Goddeeris,B., Cox,E., 2005. The role of enterocytes in the intestinal barrier function and antigen uptake. Microbes and Infection, 7, 997-1004.

Souto,E., Müller,R., 2010. Lipid Nanoparticles: Effect on Bioavailability and Pharmacokinetic Changes. In: Schäfer-Korting ,M. (Ed.), Springer Berlin Heidelberg, 115-141.

Takeuchi,H., Matsui,Y., Yamamoto,H., Kawashima,Y., 2003. Mucoadhesive properties of carbopol or chitosan-coated liposomes and their effectiveness in the oral administration of calcitonin to rats. Journal of Controlled Release, 86, 235-242.

Thompson,B., Sharp,P., Elliott,R., Al Mutairi,S., Fairweather-Tait,S.J., 2010. Development of a Modified Caco-2 Cell Model System for Studying Iron Availability in Eggs. J. Agric. Food Chem., 58, 3833-3839.

U.S. FDA Code of Federal Regulations. Title 21, Volume 3. Revised as of April 1, 2013. CITE: 21CFR184.1090 [48 FR 52445, Nov. 18, 1983, as amended at 50 FR 49536, Dec. 3, 1985; 69 FR 24512, May 4, 2004.
http://www.accessdata.fda.gov/scripts/cdrh/cfdocs/cfcfr/CFRSearch.cfm?fr=184.1090

Wang,Y., Zhu,L., Dong,Z., Xie,S., Chen,X., Lu,M., Wang,X., Li,X., Zhou,W., 2012. Preparation and stability study of norfloxacin-loaded solid lipid nanoparticle suspensions. Colloids and Surfaces B: Biointerfaces, 98, 105-111.

Xia,S., Xu,S., 2005. Ferrous sulfate liposomes: preparation, stability and application in fluid milk. Food Research International, 38, 289-296.

Yang,S., Zhu,J., Lu,Y., Liang,B., Yang,C., 1999. Body Distribution of Camptothecin Solid Lipid Nanoparticles After Oral Administration. Pharmaceutical research, 16, 751-757.

Yu,B., Zhang,Y., Zheng,W., Fan,C., Chen,T., 2012. Positive Surface Charge Enhances Selective Cellular Uptake and Anticancer Efficacy of Selenium Nanoparticles. Inorg. Chem., 51, 8956-8963.

Yuan,H., Chen,J., Du,Y.Z., Hu,F.Q., Zeng,S., Zhao,H.L., 2007. Studies on oral absorption of stearic acid SLN by a novel fluorometric method. Colloids and Surfaces B: Biointerfaces, 58, 157-164.

Zara,G.P., Cavalli,R., Bargoni,A., Fundarò.,A., Vighetto,D., Gasco,M.R., 2002. Intravenous Administration to Rabbits of Non-stealth and Stealth Doxorubicin-loaded Solid Lipid Nanoparticles at Increasing Concentrations of Stealth Agent: Pharmacokinetics and Distribution of Doxorubicin in Brain and Other Tissues. J Drug Target, 10, 327-335.

Zhang,Q., Yie,G., Li,Y., Yang,Q., Nagai,T., 2000. Studies on the cyclosporin A loaded stearic acid nanoparticles. International Journal of Pharmaceutics, 200, 153-159.

Zimmermann,M.B., Hurrell,R.F., 2007. Nutritional iron deficiency. Lancet, 370, 511-520.

Zariwala, M.G., Somavarapu,S., Farnaud, S., Renshaw, D. Comparison study of oral iron preparations using a human intestinal model. Sci Pharm; in press. doi:10.3797/scipharm.1304-03.

Captions for illustrations

Table 1. Composition of solid lipid nanoparticle (SLN) formulations.

Table 2. Physiochemical properties of solid lipid nanoparticles (SLN). All values are mean ± SD (n = 3).

Fig. 1. Effect of initial iron concentration (% w/w lipid) upon solid lipid nanoparticle (SLN) iron incorporation efficiency. Results are expressed as mean ± SD (*n* =3). ** signifies $p < 0.01$ and * signifies $p < 0.05$.

Fig. 2. Effect of chitosan inclusion on solid lipid nanoparticle (SLN) iron incorporation efficiency. Results are mean ± SD (*n* = 3). * indicates significant difference from chitosan free SLN.

Fig. 3. Transmission electron microscopy (TEM) image of iron loaded SLN-Chi-FeB visualised at 46,000x magnification.

Fig. 4. Thermal analysis of solid lipid nanoparticles (SLN's). A: DSC thermograms of stearic acid and blank SLN. B: DSC thermogram of ferrous sulphate ($FeSO_4$) loaded SLN formulations (SLN-FeA, SLN-FeB, and SLN-FeC).

Fig. 5. SLN cytotoxicity analysis. Caco-2 cells viability was assessed by MTT assay following incubation with SLN formulations for 48 and 72 h at varying iron concentrations (20 μM, 50 μM and

100 μM), with corresponding blank SLN formulations included at equivalent volumes. Results are mean ± SD (n = 6).

Fig. 6. Caco-2 cell iron absorption from test SLN formulations. Results are shown as mean ± SD (n = 6), * indicates a significant difference between ferrous sulphate control and SLN-FeA ($p < 0.05$). † indicates significant difference between SLN-FeA and SLN-Chi-FeB ($p < 0.05$).